

Design and Fabrication of Nanostructures Silicon Photodiode

Alwan M. Alwan (Corresponding author) & Allaa A. Jabbar

School of Applied Sciences, University of Technology, Baghdad, Iraq

E-mail: alkrzsm@yahoo.com

Abstract

A highly sensitive (metal/nanostructure silicon /metal) photodiode has been fabricated from rapid thermal oxidation (RTO) and rapid thermal annealing (RTA) processes, of nanostructure porous silicon prepared by laser assisted etching.

Photoresponse was investigated in the wavelength range (400-850nm). A responsivity of (3A/W) was measured at (450 nm) with low value of dark current of about ($1 \mu\text{A}/\text{cm}^2$) at 5 volt reverse bias.

Keywords: Porous silicon, Photoelectrochemical etching, Dark current, Photocurrent, Sensitivity, XRD

1. Introduction

Since the discovery of effective visible photoluminescence (PL) at room temperature from highly porous silicon (psi), a great deal of attention has been paid to its electronic properties because of the potential applications in Si-based optoelectronics (O. Klima, P. Hlinomaz, A. Hospodkova, J. Oswald, and J. Kocka. 1993) (P. Hlinomaz, O. Klima, A. Hospodkova, E. Hulicius, J. Oswald, E. Sipek, and J. Kocka, 1994); (psi) has many unique characteristics such as direct and wide modulated energy band gap, high resistivity, vast surface area-to-volume ratio and the same single-crystal structure as bulk silicon. Those advantages make it a suitable material for photodetectors (Nobuyoshi Koshida and Hideki Koyama. 1992) (Zhiliang Chen, Gijs Bosman and Romulo Ochoa. 1993).

(Psi) photodetector manufactured through conventional method is found to have several shortcomings, such as unstable optical and electrical characteristics, insufficient light sensitivity, insufficient low dark-current and insufficient photo-current, hence the application range for (psi) photodetectors is somewhat limited (Ming-Kwei Lee. 1998).

According to the paper published in 1992 by Petrova-Koch et al, it was noted that (psi) surface also contains unstable Hydrogen-passivated surface as they tend to form recombination centers that would reduce the life time of the carriers, which further reduce the (psi) photodetector's photo-current and light sensitivity and causes instability to (psi) photodetectors. (RTO) and (RTA) are utilized to improve the stability of (psi) photodetector, enhance photodetector's photo-current, and reduce dark-current of photodetectors at the same time and extend the application of (psi) photodetectors (M. K. Lee, Y. H. Wang, and C. H. Chu. 1994).

2. Experimental

The samples were prepared using silicon wafers, (111) oriented, with n-doping, and resistivity of ($1.5\text{-}4.5 \Omega\cdot\text{cm}$), $508 \mu\text{m}$ thickness. After cutting into ($1 \times 1.5 \text{ cm}^2$) specimens and standard cleaning steps, we prepared porous silicon structures by photoelectrochemical etching (PECE). In this technique the samples are dipped into a mixture of HF:Ethanol (1:1) for 20 minutes with anodization current density that was varied from 10 to $40 \text{ mA}/\text{cm}^2$. In order to achieve significant hole current in n-type silicon, external illumination was used (Red 650 nm). Typical (PECE) apparatus are schematically shown in Fig (1).

The porous layer was then rapid-thermal-oxidized (750°C , 50 sec) to form partial SiO_2 -layer and subsequently rapid-thermal-annealed at 750°C for 15 sec.

The (RTO) system as shown in figure (2) was built in laboratory and it consists of tungsten halogen photo optic lamp at 1000 Watt power. The as-prepared samples were introduced into quartz tube and the etched side was positioned directly above the halogen lamp. The quartz tube is open for allowing air to enter (dry oxygen source).

The (RTA) system as shown in figure (3) was also built in laboratory. The (RTA) system allows tungsten lamp annealing by swiftly raising the temperature to reach 750°C in 15 sec. It consists of a small vacuum chamber (quartz tube) pumped by an ordinary rotary pump (minimum pressure reached is about $10\text{-}2 \text{ torr}$). Annealing is carried out by placing the sample (etching side) on the tube directly above the lamp. There is also a thermocouple placed at the end of the tube and attached to the surface of the sample. When the temperature reads 750°C , the power is turned off and sample is allowed to cool. Finally it is removed when the temperature reads room temperature.

3. Results and Discussion

Figure (4) shows the dark current of PSi photodetector (before RTO and RTA processes) via preparation current density. We can see that the dark current decreased from ($1660 \mu\text{m}/\text{cm}^2$) at etching current density $10 \text{ mA}/\text{cm}^2$ and reached to smaller value ($1 \mu\text{m}/\text{cm}^2$) at etching current density $30 \text{ mA}/\text{cm}^2$. The decrease in dark current for four etching current density is due to decrease in thermally generated carriers so that the conductivity and dark current were reduced. We could observe the increase in dark current at etching current density $40 \text{ mA}/\text{cm}^2$. It could be caused by the defects or tunneling centers (M.Lee, Y.Wang and C.Chu. 1997).

We observed decreasing dark current with increasing etching current density after rapid thermal oxidation and rapid thermal annealing processes as shown in Fig (5), and at etching current density ($40 \text{ mA}/\text{cm}^2$), the dark current varied from ($2600-3$) $\mu\text{m}/\text{cm}^2$. That decrease is due to the increase of oxide thicknesses that reduce the tunneling probability of thermally generated carriers, so the dark current are reduce.

From figure (6), We found that the photocurrent at preparation current density $10 \text{ mA}/\text{cm}^2$ is higher than at $20, 30 \text{ mA}/\text{cm}^2$, that means that photocurrent decreases with increasing preparation current density because the increasing value of resistivity is due to increasing the psi layer thickness, but as shown in the same figure, there is increase in photocurrent at etching current $40 \text{ mA}/\text{cm}^2$. This may due to the excessive etching process which leads to increase of porosity of the porous silicon layer and hence improve the sensitivity of the formed junction between the crystalline silicon and the Psi layer.

Figure (7) shows the current–voltage curve. Typical diode behavior can be seen. When illuminated with white light, the current for reverse bias of less than -1 V is increased about thirteen orders of magnitude demonstrating the high sensitivity of the photodetector (L. A. Balagurov, S. C. Bayliss, S. Y. Adrushin, A. F. Orlov, B. Unal, D. G. Yarkin, and E. A. 2001).

Generally the forward current shows presence of distinguish stable region. First region at low voltage ($V_f < 1 \text{ volt}$), the recombination current is dominant, because the concentration of charge carriers is greater than the concentration of intrinsic ($n_p > n_i$), therefore for equilibrium case recombination process will take place, this means that each excitation electron from valance band to conduction band will recombine with a hole in valance band. Second region at high voltage ($V_f > 1 \text{ volt}$) shows forward current increase exponentially with the applied voltage because the applied voltage exceeds the potential barrier. This voltage gives the electron enough energy to overcome the barrier height and that is what called diffusion current (V.A. Vikulov V.V. Korobtsov. 2009). In the reverse bias, also there are two regions, one at low voltage, where the current increases with the applied voltage and the generated current is dominant. In the second region, the current is dependent on voltage and the diffusion current is dominant.

Figure (8) illustrates the measured sensitivity (R_s) as a function of various incident wavelengths. From this figure (8) we can see that the spectral responsivity of structures measured in the wavelength range from (400-850) nm. We notice that the observed photo responsivity is shifted towards shorter wavelength in agreement with the assumption that the emission is related to quantum size effects (A.Akram. 2008). For longer wavelengths (700-900)nm, we can see that the value of responsivity decreased away from the responsivity top, that decrease in responsivity is attributed to the incident photon energy not being enough to generate electron–hole pairs (M.Lee, Y.Wang and C.Chu. 1997).

This large variation in the sensitivity with the incident photo energy is due to the variation in absorption depth which is a function of wavelength of the incident light, where the absorption of short wavelength occurs within the (Psi) layer and the large wavelength is absorbed at the interface of silicon and (Psi) (Svechnikov S.V., Kaganovich E.B., and Manoilv E.G, Semicond. 1998).

Figure (9) shows the X-ray diffraction of PSi at $30 \text{ mA}/\text{cm}^2$ etching current density. From this measurement, we can observe apparent new small peak at new diffraction angle, this may be attributed to new nanostructure which was different in morphology.

The morphological phase of nano (PSi) layer (crystalline or amorphous) will give good concept for electrical behavior of this material (P. Balk. 1965). The nanocrystallite size can be calculated by employing Scherer's formula as shown in the equation below:

$$L = \frac{0.9\lambda}{B \cos \theta_B}$$

Where L is the nanocrystallite size for PSi layer in (nm), λ is the wavelength in (nm) of employed radiation, B (radians) is the full width half maximum (FWHM), θ_B (radians) is the diffraction angle and 0.9 is the value of shape factor (B. D. Cullity. 1967).

The morphological properties of the porous silicon sample prepared at current 30mA/cm² is shown in figure (10). From this figure, we can see that the pore size varied from (0.1~1µm), while the average silicon sizes in the porous layer is less than (0.4 µm).

4. Conclusion

In this paper, the treatments of RTO and RTA processes have been used to enhance the photoresponsivity and reduce the dark current to (3 µA /cm²) at preparation current density (40 mA/cm²). The device is very stable and the reproducibility is good due to a stable surface on the PS layer and it can be concluded from I-V characteristic, of our devices which shows rectifying behavior.

The optimized RTA-RTO-PS photodetector has the performance of temperature 750°C (under 100 mW/cm illumination). A high response of 3 A/W can be obtained under a 5W (810 nm) laser diode illumination.

Acknowledgment

This work was supported and sponsored in part by the School of Applied Sciences/UOT/Baghdad-IRAQ.

References

- A.Akram. (2008). Thesis, RTO effect on PS prepared by Stain Etching, Univ. Technology, Iraq, (2008).
- B. D. Cullity. (1967). *Elements of X-Ray diffraction*, Addison-Wesley Publishing, Company, Inc. America, (1967).
- L. A. Balagurov, S. C. Bayliss, S. Y. Adrushin, A. F. Orlov, B. Unal, D. G. Yarkin, and E. A. (2001). Petrova, Solidstate Electron. 4, 1607 (2001).
- M. K. Lee, Y. H.Wang, and C. H.Chu. (1994). High-Sensitivity Porous Silicon Photodetectors Fabricated Through Rapid Thermal Oxidation and Rapid Thermal Annealing. *IEEE journal of quantum electronics*, VOL.33, NO 12, Decembr(1994).
- M.Lee,Y.Wang and C.Chu. (1997). IEEE QE.33 (12)(1997)2199.
- Ming-Kwei Lee. (1998). National Science Council,Taiwan. METHOD TO IMPROVE THE SHORT CIRCUTE OF THE POROUS SILICON PHOTODETECTOR Mar. 13, 1998 .
- Nobuyoshi Koshida and Hideki Koyama. (1992). Visible electroluminescence from porous silicon, *Appi. Phys. Lea.*, Vol. 60, pp. 347-349, Jan 1992.
- O. Klima, P. Hlinomaz, A. Hospodkova, J. Oswald, and J. Kocka. (1993). *J. of Non-Cryst. Solids*, 961, pp. 164 ñ 166 (1993).
- P. Balk. (1965). *The Electrochem. Soc. Meeting*, Buffalo, NY, Oct. 10-14, 1965.
- P. Hlimonaz, O. Klima, A. Hospodkova, E. Hulicius, J. Oswald, E. Sipek, and J. Kocka. (1994). *Appl. Phys. Lett.*, 64, p. 3118 (1994).
- Svechnikov S.V., Kaganovich E.B., and Manoily E.G, Semicond. (1998). *Phys. Quan. & Optoelc.* 1, 1998,P.13
- V.A. Vikulov V.V. Korobtsov. (2009). Thin Solid Films, Elsevier B.V. Elsevier B.V. 517, 3912–3915, 4 February, (2009).
- Zhiliang Chen, Gijs Bosman and Romulo Ochoa. (1993). Visible light emission from heavily doped porous silicon homojunction pn diodes, *Appl. Phys. Lett.*, Vol. 62, pp.708-710, Feb 1993.

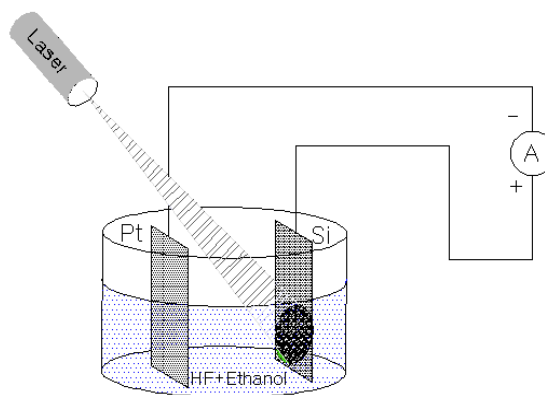


Figure 1. Schematic diagram of the photoelectrochemical etching system

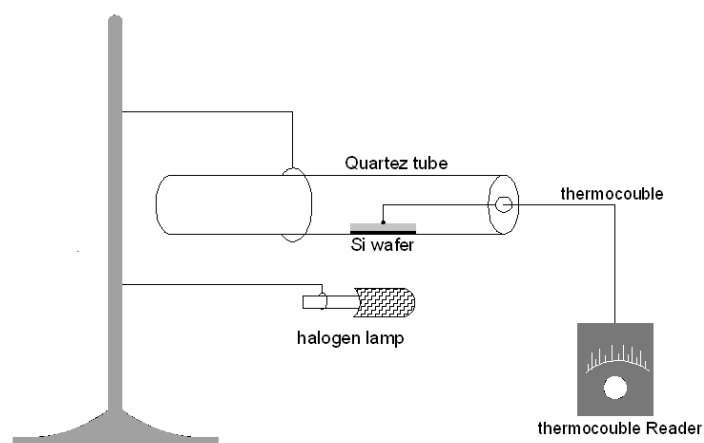


Figure 2. Schematic diagram of rapid thermal oxidation system

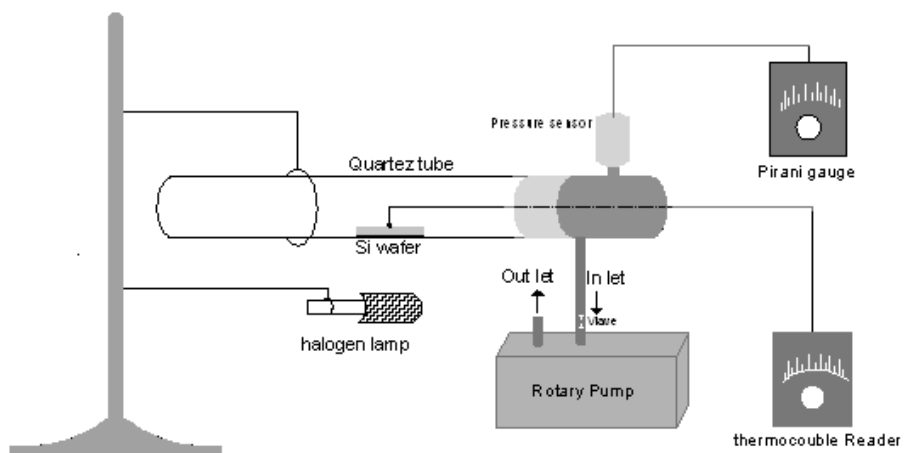


Figure 3. Schematic diagram of the rapid thermal annealing system

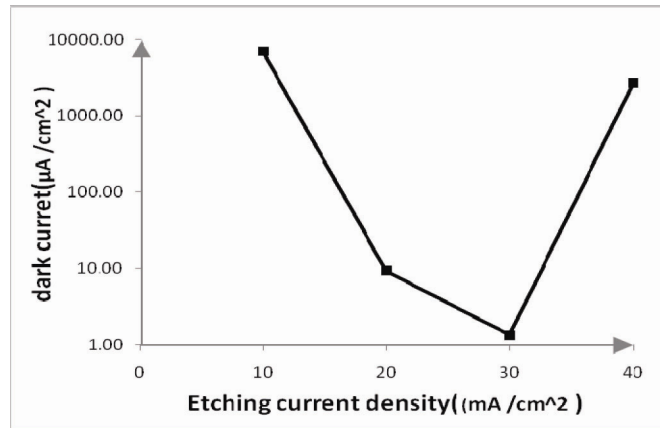


Figure 4. the dark current at different etching current density (10, 20, 30, 40 mA/cm²), under reverse bias 5V

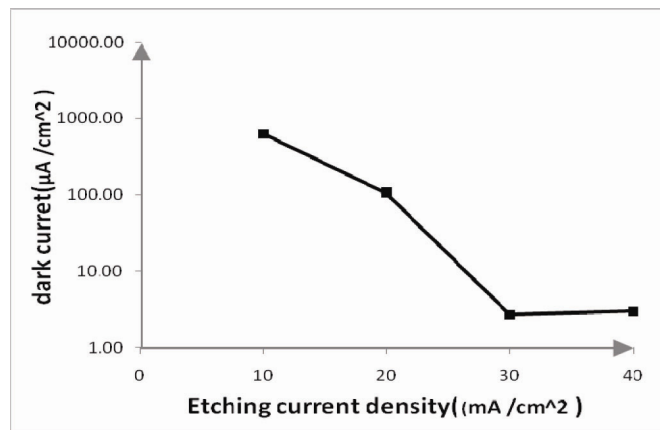


Figure 5. the dark current at different etching current density (10,20,30,40 mA/cm²), after RTO and RTA processes,(100 sec) and (15 sec) sequently, under reverse bias 5V

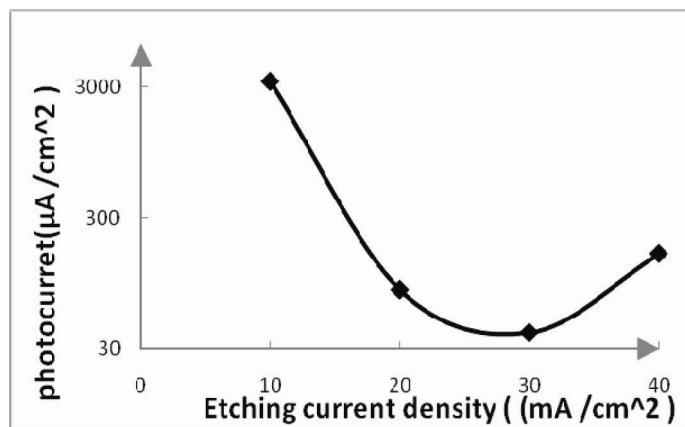


Figure 6. shows the variation of photo current as a function to the preparation current density at specific illumination power 200mW/cm²

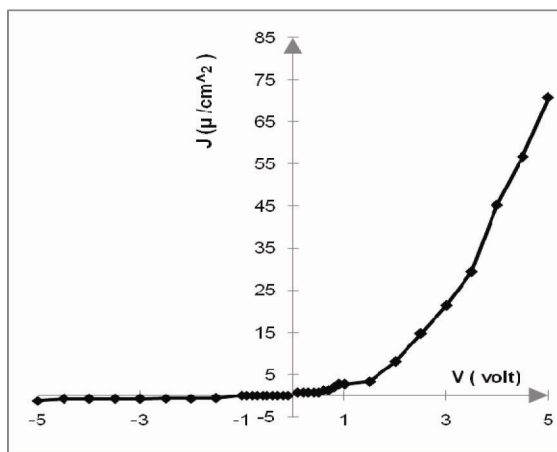


Figure 7. the (I – V) characteristics for (metal/nanostructure silicon /metal) photodiode at etching current density (30 mA/cm^2), under reverse bias 5V and illumination power 200 mW/cm^2

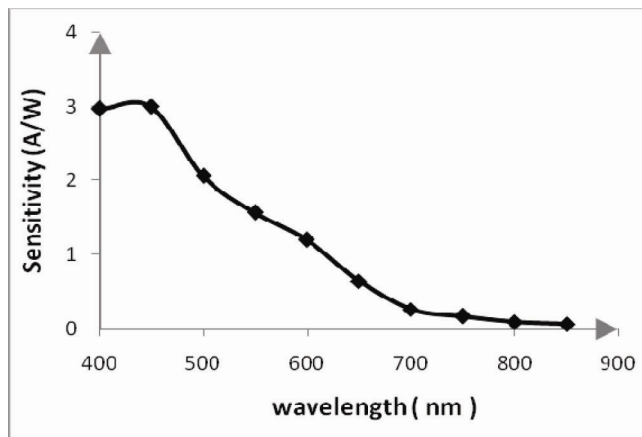


Figure 8. the sensitivity as a function of various wavelength (400-850)nm ,for Psi sample prepared at (30 mA/cm^2)

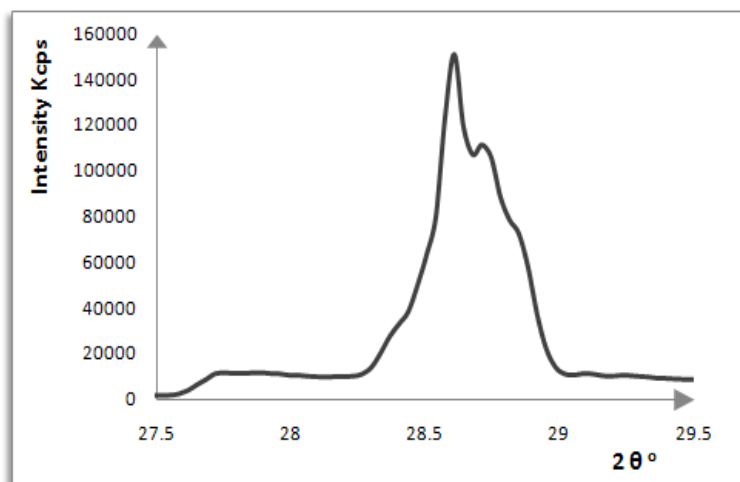


Figure 9. X-ray diffraction for porous silicon at 30 mA/cm^2 etching current density

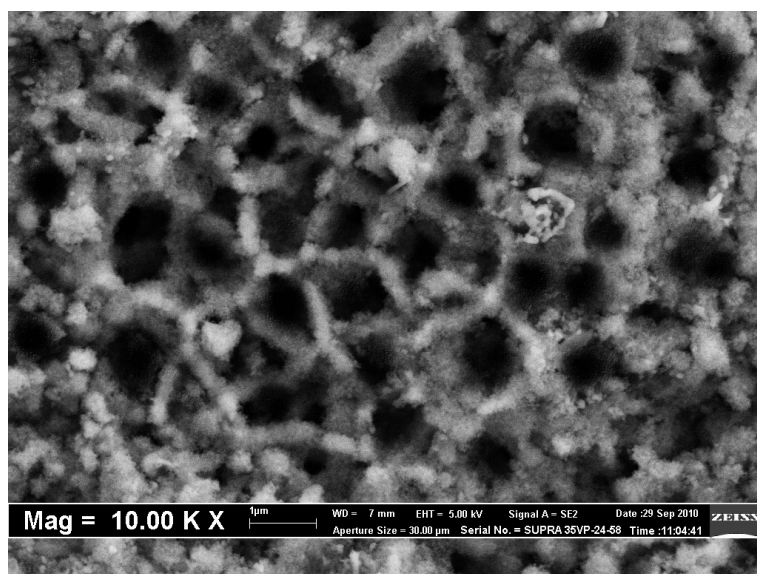


Figure 10. the SEM image of porous silicon sample prepared at etching current of (30 mA/cm²)